

$UBV(RI)_C$ photometry of the open clusters Be 15, Be 80, and NGC 2192

M. T. Tapia^{1,2,3} *, W.J. Schuster², R. Michel², C. Chavarría-K.², W. S. Dias⁴, R. Vázquez², and A. Moitinho⁵.

¹ *Instituto Astrofísico de Canarias, E-38200, La Laguna, Tenerife, Spain*

² *Instituto de Astronomía, Universidad Nacional Autónoma de México, Ensenada 22860, Baja California, México*

³ *Universidad Autónoma de Baja California, Ensenada 22860, Baja California, México*

⁴ *UNIFEI, Instituto de Ciências Exatas, Universidade Federal de Itajubá, Itajubá MG, Brazil*

⁵ *SIM/IDL, Fac. de Ciências, Universidade de Lisboa, Ed. C8, Campo Grande, 1749-016, Lisboa, Portugal*

Accepted XXXX. Received YYYY; in original form ZZZZ

ABSTRACT

The three open clusters Be 15, Be 80, and NGC 2192 have been observed using CCD $UBV(RI)_C$ photometry at the San Pedro Mártir Observatory, México within the framework of our open-cluster survey. The fundamental parameters of interstellar reddening, distance, and age have been derived, and also the metallicity for NGC 2192 (solar metallicity has been assumed for the other two). By shifting the colours of Schmidt-Kaler in the $(U-B, B-V)$ two-colour diagram along the appropriate reddening vector, the interstellar reddenings have been derived as $E(B-V) = 0.23 \pm 0.03$ mag for Be 15, 1.31 ± 0.05 for Be 80, and 0.16 ± 0.03 for NGC 2192. Evidence is shown for a variable interstellar extinction across the cluster Be 80. For NGC 2192 a nicely consistent fit is obtained for both the interstellar reddening and the metallicity ($[Fe/H] = -0.31$) using simultaneously the F-type and red-clump stars.

By fitting isochrones to the observed sequences of these three clusters in various colour–magnitude diagrams of different colour indices, $(B-V, V-I, \text{ or } V-R)$ the averages of distance moduli and heliocentric distances ($(V-M_V)_o$ (mag); d (pc)) are the following: $(10.74 \pm 0.01; 1202)$ for Be 15, $(10.75 \pm 0.01; 1413)$ for Be 80, and $(12.7 \pm 0.01; 3467)$ for NGC 2192, and the averages of the inferred best ages ($\log(\text{age})$; age (Gyr)) are $(8.6 \pm 0.05; 0.4)$ for Be 80, and $(9.15 \pm 0.05; 1.4)$ for NGC 2192; for Be 15 there are two distinct possibilities for the age fit, depending on the membership of three brighter stars, $(9.35 \text{ or } 9.95 \pm 0.05; 2.2 \text{ or } 8.9)$. The need for spectroscopic observations in Be 15 is emphasized to select between alternate reddening and age solutions, and for deeper UBV observations in Be 80 to study in greater detail the variable interstellar, or intracluster, reddening across this cluster.

Key words: open clusters and associations: individual: Be 15, Be 80, NGC 2192 – Hertzsprung-Russell (HR) and C-M diagrams – stars: fundamental parameters – stars: distances – ISM: dust, extinction

1 INTRODUCTION

Stellar clusters are ideal for research being groups of stars born simultaneously, under the same physical conditions, situated at the same distance, but with a wide range of stellar masses. Altogether stellar clusters are excellent probes for the study of the structure, and dynamical and chemical evolutions of the Galaxy, since their interstellar reddenings, chemical abundances, distances, and ages can

be determined with precision using various colour–colour and colour–magnitude diagrams from the $UBV(RI)_C$ photometry, as well as stellar models and isochrones. In effect, the younger open stellar clusters have been utilized as tracers of spiral structure of the Galaxy (e.g. Becker & Fenkart 1970, Moffat & Vogt 1973, Feinstein 1994), as tracers of Galactic three-dimensional structure (e.g. Cabrera-Caño et al. 1990, Phelps & Janes 1994, Moitinho 2002), and in the analysis of the structure and chemical evolution of the Galactic disc (e.g. Janes 1979, Friel 1995, Piatti et al. 1995, Twarog et al. 1997). Individually, stellar

* E-mail: mtt@iac.es(MTT), schuster@astrosen.unam.mx(WJS)

clusters can be used to constrain and test the theories of stellar formation and evolution. The detailed comparison between photometric diagrams and theoretical isochrones, calculated from models of stellar evolution, has led to enormous advances in the understanding of stellar structure and evolution, and is still providing very useful information concerning the effects of convective overshooting, chemical compositions, gravitational settling, and radiative accelerations (Meynet et al. 1993, Kassis et al. 1997, Michaud et al. 2004). These photometric diagrams are also useful in searching for interesting and peculiar stars, such as Be stars, blue stragglers, recently formed stars, and the brightest red giants (Mermilliod 1982a,b; Mermilliod & Mayor 1989; Chavarría-K 1994; Moitinho et al. 2001).

In these Galactic studies, one of the more severe observational limitations is due to the absence of photometric data for nearly half of the approximately 1500 open clusters known, combined with the lack of homogeneity in the observations and analyses for those clusters which have been studied. These limitations form the crux of various controversies, such as: (1) whether or not there is a metallicity gradient as a function of the Galactocentric radius (Janes 1979, Twarog et al. 1997, Carraro et al. 1998), (2) whether or not there is a vertical metallicity gradient with respect to the Galactic disc (Piatti et al. 1995), and (3) uncertainties in the characteristics of the Galactic structure, for example the spiral structure (i.e. the number and positions of the various arms).

The catalogue of Lyngå (1987), which includes distances for 422 open clusters, has constituted the observational basis for a large number of astronomical studies, has led to important conclusions about the Galactic disc, and has been very useful for planning subsequent observations by other astronomers. However, this catalogue has been built from parameters obtained by various authors, with diverse observing techniques, distinct calibrations, and different criteria for determining the stellar ages, rendering it very inhomogeneous and limited for studies requiring precision in the measurement of these fundamental parameters. As an example of the precision and accuracy that one can expect due to the effects of these inhomogeneities, we refer to Janes & Adler (1982), who found that distance moduli obtained by two or more authors have a mean difference of 0.55 mag (see also WEBDA: <http://www.univie.ac.at/webda/navigation.html>).

To remedy these inaccuracies, a project ('A $UBV(RI)_C$ survey for open clusters of the northern hemisphere') has been developed whose principal objective is to obtain and to analyze in a systematic way a set of CCD data, taken with the $UBV(RI)_C$ photometric system, for the more than 300 open clusters visible from the National Astronomical Observatory, San Pedro Mártir (SPM), most of which have been previously unstudied (Schuster et al. 2007; Michel et al. in preparation). With this photometry, which is homogeneous regarding instrumentation, observing techniques, reduction methods, and analysis, the following will be obtained: (a) a uniform, photometric reference system via open clusters to which other photometric studies can be transformed, (b) an atlas of colour-colour (CC) and

colour-magnitude (CM) diagrams for Galactic open clusters with distinct fundamental parameters, (c) a homogeneous data set of interstellar reddenings, metallicities, distances, and ages for a large set of Galactic open clusters, (d) an increased number of old and distant open clusters. (e) selection criteria lists for subsequent spectroscopic and deeper photometric studies of open clusters.

2 THE SELECTION OF THE CLUSTERS

The open clusters for our 'quick' survey have been selected from the large (and mostly complete) catalogue of Dias et al. (2002), 'Optically visible open clusters and Candidates', which is now also available and updated through 2007 at the CDS (Centre de Données Astronomiques de Strasbourg) as catalogue VII/229 (or B/ocl). Our subset of clusters are those observable from SPM (latitude $+31^{\circ}44'$) and which have little or no previous studies, such as Be 15 and Be 80 of this paper; a few others which have been analyzed earlier have also been added for comparison purposes, such as NGC 2192 (Tapia-Peralta 2007). More details concerning the selection of clusters and the project motivation will be presented in the principal, introductory publication of this survey (Michel et al. in preparation). The three open clusters of this paper, Be 15, Be 80, and NGC 2192 represent a small, carefully selected sample used to test and to define the analysis procedures of this 'quick' survey; these clusters have been well observed, provide probable turn-offs in the G-, B-, and F-type stars, respectively, and include small to moderately large interstellar reddenings.

3 CCD OBSERVATIONS AND REDUCTIONS

A CCD $UBV(RI)_C$ survey of northern open clusters has been undertaken at SPM using always the same instrumental setup (telescope, CCD, filters), observing procedures, reduction methods, and system of standard stars (Landolt 1983, 1992). The CCD $UBV(RI)_C$ observations of this paper have been made exclusively with the 0.84-m f/13 Cassegrain telescope at SPM, during the night of 2001 June 25/26 for the open cluster Be 80, and the nights 2002 February 6/7 and 8/9 for the clusters NGC 2192 and Be 15, respectively. The telescope hosted the filter-wheel 'Mexman' with the SITe 1 (SI003) CCD camera, which has a 1024×1024 square pixel array, with a pixel size of $24\mu\text{m} \times 24\mu\text{m}$; this CCD has nonlinearities less than 0.45 per cent over a wide range, no evidence for fringing even in the I band, and Metachrome II and VISAR coverings to increase sensitivity at the blue and near-ultraviolet wavelengths. This telescope was re-focused before the observation of each open cluster, usually using the V filter of our parfocal set of $UBV(RI)_C$ filters. The open clusters have been observed with exposure times of 3×240 seconds for the U filter, 3×180 for B , 3×100 for V , 3×100 for R , and 3×120 for I ; for Be 15 and NGC 2192 extra exposures in the filter U were made to improve the signal-to-noise. Also, for Be 80 exposures as short as 10 seconds have been made in the R and I filters to de-saturate the brightest stars of the field, and as short as 25 seconds to de-saturate the brightest stars of Be 15 and NGC 2192.

Each night several standard-star fields from Landolt (1992) were observed to permit the derivation of the photometric transformations to the system of Johnson-Cousins and the coefficients of the atmospheric extinction. For the June 2001 observing run, six Landolt groups were used, containing 23 different standard stars: PG1633+099 (5 stars), MARK A (4 stars), PG1528+062 (3 stars), PG1530+057 (3 stars), PG1525-071 (4 stars), and PG1657+078 (4 stars), with a range in $(B-V)$ from -0.252 to $+1.134$, in $(U-B)$ from -1.091 to $+1.138$, and in $(V-I)$ from -0.296 to $+1.138$. Thirteen to 25 observations of these Landolt standards were made per night. For the February 2002 run eight Landolt groups were employed, containing 35 different standard stars: PG1047+003 (4 stars), PG1323-086 (5 stars), SA95 (5 stars), SA107 (4 stars), PG0942-029 (5 stars), SA104 (4 stars), PG0918+029 (5 stars), and PG1528+062 (3 stars), with a range in $(B-V)$ from -0.294 to $+1.412$, in $(U-B)$ from -1.175 to $+1.265$, and in $(V-I)$ from -0.280 to $+1.761$. Fifty-two to 72 observations of these Landolt standards were made per night, except one night cut short by clouds, when only 15 observations were managed. The standard-star fields have been observed with exposures of 1×240 seconds for the U filter, 1×120 for B , 1×60 for V , 1×60 for R , and 1×60 for I .

Usually one, or more, Landolt fields were re-observed with an air-mass range of at least 0.70 in order to measure the coefficients of the atmospheric extinction. For example, the night when Be 80 was observed, an approximate air-mass range of 1.29 was achieved, and a range of 1.26 for NGC 2192. Due to the wide band-passes of these Johnson-Cousins filters, second-order colour terms were included in these atmospheric-extinction corrections. For the large air-mass observations required for an atmospheric-extinction determination, the filters were frequently observed with both forward and backward sequences (i.e. *UBVRIRVB*); this was occasionally done also for other standard-star fields to increase the accuracy, precision, and observing efficiency of the photometric observations.

The usual calibration procedures for CCD photometry have been carried out during each of our observing runs. Fifty to a hundred ‘bias’ exposures have been made each night, and fifty or more ‘darks’ during each run with exposures of 4–15 minutes, according to the longest of our stellar exposures; these ‘darks’ were usually made during the non-photometric nights. Flat fields were obtained at the beginning and end of the nights by observing a clear patch of sky; at least 5 flat fields were obtained for each filter per night with exposures greater than 5 seconds, and with small offsets on the sky between each flat-field exposure.

The data reductions of this CCD photometry have been carried out using the usual techniques and packages of IRAF.¹ Aperature photometry and PSF photometry have been used for handling the standard-star and cluster-star observations, respectively (Howell 1989, 1990; Stetson 1987, 1990). More details concerning the instrumentation and the observing and reduction procedures of this project will be given in an introductory paper (Michel et al. in preparation).

For the analyses of these open clusters, an awk macro, ‘elipse’, has been developed which allows us to concentrate on the centre of a cluster, as defined by visual inspection in a visual (V) or red (R) image, helping to increase the contrast of the cluster with respect to the surrounding fields in the various colour-colour (CC) and colour-magnitude (CM) diagrams. This macro defines an elliptical area on the image, and when applied to the CCD data file, retains all stars within this elliptical area for further analyses and excludes all stars outside this area. The input parameters of this macro are the centre of the ellipse (X, Y coordinates in pixels), the major and minor axes of the ellipse in pixels, and an angle of rotation in degrees. This macro has been used interactively by selecting the input parameters, then plotting the resulting elliptical field, and finally iterating to a more concentrated central region as seen in the visual or red image. This ellipse has been fit as tightly as possible to each cluster while still including all obvious visible members. This process is somewhat subjective, and has been applied prior to the plotting of any CC or CM diagrams.

A java-based computer program (‘SAFE’ by J. McFarland, 2009) has also been utilized for the visualization and analysis of the photometric data of these open clusters (Schuster et al. 2007). This system is capable of displaying each cluster’s data simultaneously in different CC and CM diagrams and has an interactive way to identify a star, or group of stars, in one diagram and to see where it falls in the other diagrams, thus facilitating the elimination of field stars and the apperception of cluster features. This program is capable of displaying up to 16 different diagrams for one cluster while processing up to 20 clusters at the same time.

X and Y positions (in pixels), and standard *UBVRI* CCD photometry and observing errors for the open clusters Be 15, Be 80 and NGC 2192 are presented in Tables 1–3, respectively.

4 BERKELEY 15

Be 15 is located in the constellation Auriga, in the Galactic anti-centre direction ($\ell, b = 162.27^\circ, +01.61^\circ$), has an apparent diameter of about 5.0 arcmin (Lyngå 1987), and was classified as II-2-p by Trumpler (1930) and reclassified as I-2-m by Lyngå (1987), indicating a medium to poor cluster ($\lesssim 50$ – 100 stars) with a moderate central condensation, and a medium luminosity contrast with respect to the surrounding fields. Lyngå (1987) gives ≈ 15.0 mag as the visual magnitude of its brightest star, and this cluster has also been designated as OCl 414 and C 0458+443 in Simbad.

For the cluster Be 15, the macro ‘elipse’ has been used to retain a nearly circular region for the photometric analyses (see Fig. 1): the centre at (487, 482) pixels; a north-south axis of 256 pixels (1.68 arcmin); an east-west axis of 259 pixels (1.70 arcmin); and a position angle of $+85^\circ$. The total field of view of the SITe1 CCD at the 0.84-m telescope is 6.72×6.72 square arcmin.

4.1 Colour-colour diagram, $(U-B)$ versus $(B-V)$

The $(U-B)$ versus $(B-V)$ diagram of this open cluster is presented in Fig. 2 together with the Schmidt-Kaler (1982)

¹ IRAF is distributed by NOAO, which is operated by the Association of Universities for Research in Astronomy, Inc., under cooperative agreement with the NSF

Table 1. Standard *UBVRI* CCD photometry and observing errors for the open cluster Be 15. The columns give successively the following: X and Y (pixels), the position of a star in the CCD field; *U*, *B*, *V*, *R*, and *I* (magnitudes), the standard photometry of this star; and σ_U , σ_B , σ_V , σ_R , and σ_I (magnitudes), photometric errors as provided by IRAF. Values of ‘99.999’ indicate photometry that was not measurable, mainly due to faintness in the ‘U’ or ‘B’ bands or due to image defects. This is a sample of the full table which is available in the online version of the article.

X	Y	U	B	V	R	I	σ_U	σ_B	σ_V	σ_R	σ_I
126.1	17.2	16.025	14.581	12.981	12.113	99.999	0.012	0.002	0.003	0.020	99.999
67.8	18.5	18.052	17.490	16.470	15.902	15.130	0.016	0.006	0.004	0.003	0.003
91.4	33.5	16.783	16.419	15.383	14.752	13.990	0.012	0.001	0.002	0.003	0.001

Table 2. The same as Table 1 but for Be 80. This is a sample of the full table which is available in the online version of the article.

X	Y	U	B	V	R	I	σ_U	σ_B	σ_V	σ_R	σ_I
560.3	19.5	17.364	16.915	15.490	14.534	13.453	0.044	0.001	0.002	0.002	0.003
806.4	28.6	19.120	18.482	17.101	16.204	15.169	0.292	0.022	0.004	0.007	0.003
172.6	37.1	99.999	99.999	18.994	17.176	15.362	99.999	99.999	0.032	0.012	0.007

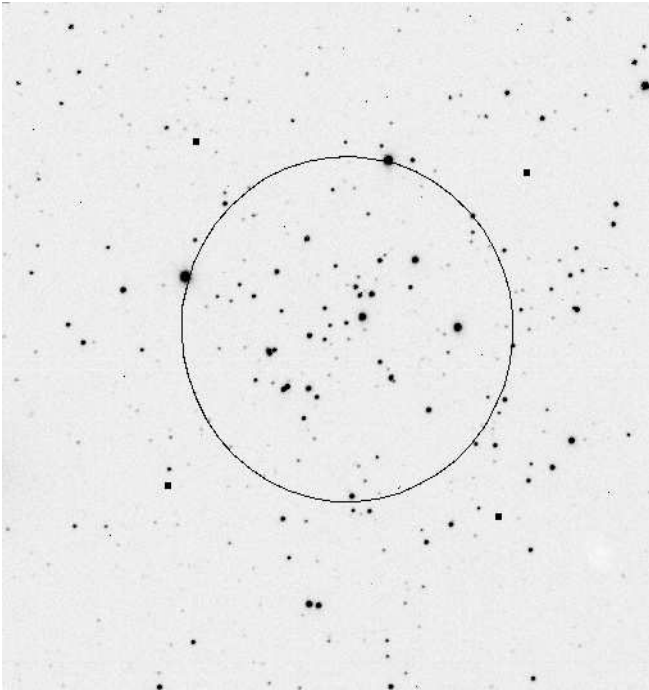


Figure 1. Visual image of the open cluster Be 15 as seen on the DPSS. The nearly circular region encloses those stars studied in this publication; details are given in the text. North is up, and east to the left in this image

main-sequence colours, which have been fit assuming G-type stars, providing an interstellar reddening of $E(B-V) = 0.23 \pm 0.03$ mag for Be 15. Only stars with photometric errors less than 0.10 mag for the ($U-B$) colour have been plotted to compensate for the low sensitivity of this CCD in the ultraviolet. The observed slope of these stars in Fig. 2 fits much better the Schmidt-Kaler G-type main-sequence colours, which are more vertical. Another study, mentioned below, has fit the observed stars to these B-type colours. Photometric error bars, and the reddening vector corresponding to $E(B-V) = +0.23$ are also shown in Fig. 2. At the redder colours the points begin to scatter more due to increasing photometric errors in ($U-B$) and ($B-V$), possi-

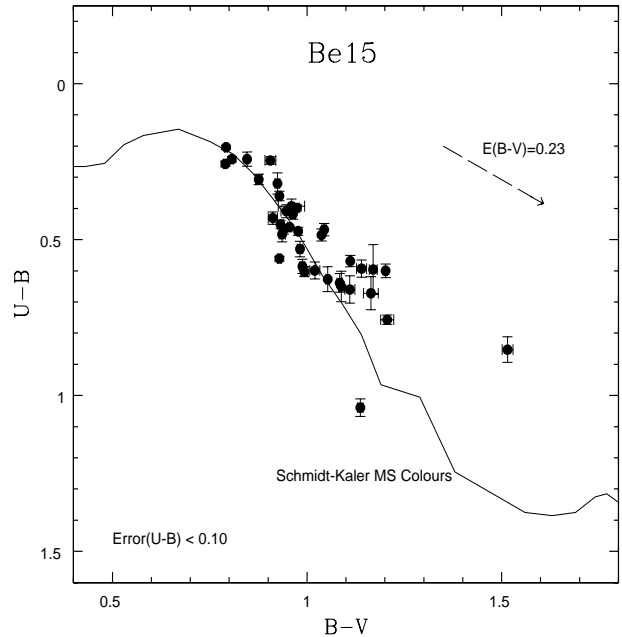


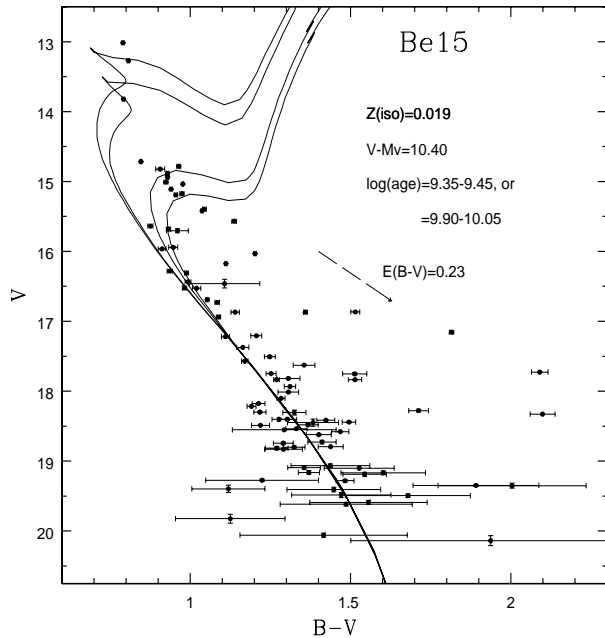
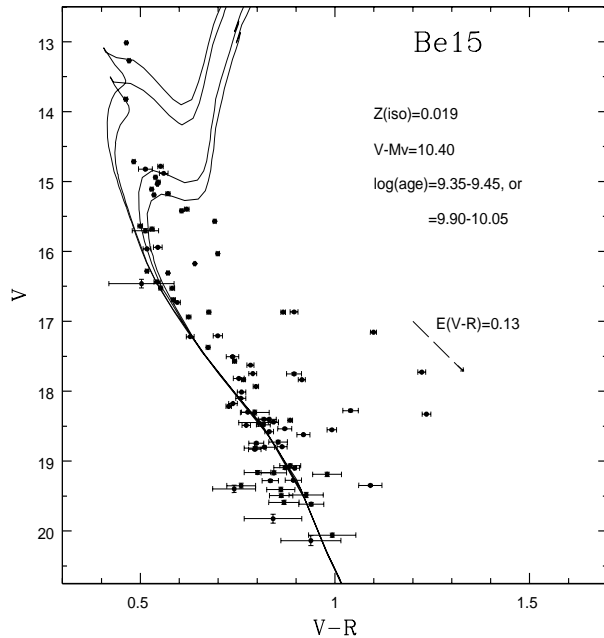
Figure 2. The CC, ($U-B$) vs ($B-V$), figure for the open cluster Be 15. This cluster has been fit to the main-sequence colours of Schmidt-Kaler (1982), the thick solid line which crosses the diagram from upper left to lower right. Only stars with photometric errors less than 0.10 mag for the colour ($U-B$) have been plotted. Photometric error bars, and the reddening vector corresponding to $E(B-V) = +0.23$ are also shown

ble binary stars, and also due to the probable inclusion of background stars with greater interstellar reddening. Since this is an older cluster lacking F-type stars, no means for estimating an ultraviolet excess, $\delta(U-B)$ or $\delta_{0.6}$, is available, and so a solar metallicity, $Z = 0.019$, has been assumed for Be 15.

Lata et al. (2004) also studied Be 15 in this same ($U-B$) versus ($B-V$) diagram from CCD *UBVRI* photometry, but they fitted to the B-type main-sequence stars of Schmidt-Kaler (1982) obtaining a reddening of $E(B-V) = +0.88$, much larger than our result. In support of our interstel-

Table 3. The same as Table 1 but for NGC 2192. This is a sample of the full table which is available in the online version of the article.

X	Y	U	B	V	R	I	σ_U	σ_B	σ_V	σ_R	σ_I
637.9	13.7	18.589	18.475	17.739	17.333	16.859	0.024	0.032	0.011	0.008	0.015
935.5	20.9	18.546	18.569	17.892	17.485	17.018	0.036	0.015	0.023	0.010	0.009
640.6	25.0	17.145	17.112	16.491	16.176	15.790	0.012	0.006	0.002	0.006	0.005


Figure 3. The CM figure, ($V, B-V$), for the open cluster Be 15. This cluster has been fit to the isochrones of Girardi et al. (2000) according to the interstellar reddening determined above in the CC diagram of Fig. 2, $E(B-V) = +0.23$; $[Fe/H] = 0.00$ dex has been assumed. The distance modulus of Be 15 has been determined by fitting vertically the cluster to the isochrones at the intermediate magnitudes of the main sequence, $16.5 \lesssim V \lesssim 18.5$ mag, and the age by fitting the turn-off of the cluster at the brighter magnitudes, $13.0 \lesssim V \lesssim 16.0$; two possible ages solutions are suggested depending on the membership of three brighter stars. Photometric error bars, and the reddening vector corresponding to $E(B-V) = +0.23$ mag are also shown

Figure 4. The CM figure, ($V, V-R$), for the open cluster Be 15. This cluster has been fit to the isochrones of Girardi et al. (2000) according to the interstellar reddening determined above in the CC diagram of Fig. 2, $E(B-V) = +0.23$ mag; $[Fe/H] = 0.00$ dex has been assumed. Other details as in Fig. 3

lar reddening estimate, the interstellar extinction maps of Neckel & Klare (1980) indicate $A_V \approx 0.80$ mag, according to their Figs 5b and 6c, for the Galactic longitude and latitude of Be 15, and for the distance derived in our next Section 4.2 ($d \approx 1.2$ kpc). This visual absorption corresponds to $E(B-V) \approx +0.28$ mag, much closer to our result than to that of Lata et al. (2004). In addition, the reddening value of Be 15 has been derived from the dust maps of Schlegel, Finkbeiner & Davis (1998; hereafter, SFD), which are based on the *COBE/DIRBE* and *IRAS/ISSA* maps and take into account the dust absorption all the way to infinity. A $E(B-V)(\ell, b)_\infty$ value of 1.22 for Be 15 has been taken from SFD maps using the web pages of NED². This value to infinity has been reduced slightly according to the

corrections discussed in Arce & Goodman (1999), Bonifacio, Monai & Beers (2000), and Schuster et al. (2004). Then the final reddening for a given star is reduced again by a factor $\{1 - \exp[-d \sin |b|/H]\}$, where b , d , and H are the Galactic latitude, the distance from the observer to the object, and the scale height of the dust layer in the Galaxy, respectively; $H = 125$ pc has been assumed here (Bonifacio, Monai & Beers 2000). For Be 15 this estimated interstellar reddening works out as $E(B-V) = +0.24$, again much closer to our value than to that of Lata et al. (2004). However, the 3 kpc distance of Lata et al. (2004) is also much larger than ours leading to larger A_V and $E(B-V)$ values from Neckel & Klare and from SFD, ≈ 2.5 mag, i.e. $E(B-V) \approx +0.81$ mag (good agreement with Lata et al.'s result), and 0.49 mag (not so good agreement), respectively. So, we prefer our small reddening solution due to the better fit to the slope of the Schmidt-Kaler colours in Fig. 2, and also due to more consistent fits to the results from **both** Neckel & Klare and SFD.

Sujatha et al. (2004) have also studied Be 15 using *UBVRI* CCD photometry, and have employed the ($B-I$) vs ($B-V$) diagram plus the technique given by Natali et al. (1994) obtaining an interstellar reddening of $E(B-V) =$

² <http://nedwww.ipac.caltech.edu/forms/calculator.html>

0.462 mag, larger than our value. But, their distance modulus and distance are in good agreement with our estimates: 10.5 mag and 1259 ± 135 pc (Sujatha et al. 2004) compared to 10.4 mag and 1202 ± 50 pc (our values, next section), providing confidence in our smaller reddening estimate from Fig. 2, and also in the smaller estimates from Neckel & Klare and SFD, which depend on this distance.

4.2 Colour–magnitude diagrams

In Figs 3 and 4 are shown the CM diagrams, $(V, B-V)$ and $(V, V-R)$, respectively, employed for Be 15 to determine its distance and age. In these CM diagrams the observations have been fit to the isochrones of Girardi et al. (2000) using the interstellar reddening determined above, $E(B-V) = 0.23$ mag, which converts to $A_v = 0.71$ mag, assuming $R_V = 3.1$, and $E(V-R) = 0.13$ mag, according to the reddening ratios found in Straizys (1995), $E(V-R) = 0.56E(B-V)$. Solar metallicity has been assumed.

For both these CM diagrams the distance moduli have been determined by shifting the reddening-corrected isochrones vertically to fit the observed V magnitudes at intermediate values, $16.5 \lesssim V \lesssim 185$ mag. At these intermediate magnitudes the cluster main sequence is more inclined (i.e. less vertical) than at the brighter magnitudes, but still with fairly small photometric errors, allowing an accurate fit. Both diagrams give a distance modulus of $(V-M_V)_o = 10.4$ mag with an estimated uncertainty of about ± 0.1 mag. Likewise, both diagrams have been used to estimate the cluster ages by fitting the cluster turn-offs to the isochrones at the brighter magnitudes, $13.0 \lesssim V \lesssim 16.0$ mag. Both CM diagrams indicate a rather large uncertainty in the cluster age, depending on whether the three brightest stars, $V \approx 13.5$ mag, are members or not. For this reason two possible age solutions are indicated in each CM diagram, both with a pair of isochrones. In both cases the younger age solution corresponds to $\log(\text{age}) \cong 9.35\text{--}9.45$ by fitting to these three brightest stars, and an older solution to $\log(\text{age}) \cong 9.90\text{--}10.05$ by fitting to a clump of apparent turn-off stars about 1.5 mag fainter. The double isochrones plotted help to appreciate the uncertainties in these (logarithmic) age estimates, $\approx \pm 0.05$ dex. In Figs 3 and 4, photometric error bars, and the reddening vector corresponding to $E(B-V) = +0.23$ mag are also shown. The results from these two CM diagrams concerning the distance modulus and age are very consistent. A definitive age for Be 15 from our CCD photometry must await radial velocity and/or proper motion studies to determine the membership, or not, of the brightest stars in the field of Be 15.

As mentioned above, the results of Sujatha et al. (2004) agree very well with ours. They obtain a distance modulus of 10.5 mag, and $\log(\text{age}) \approx 9.7$. On the other hand, Lata et al. (2004) obtain a large-distance/small-age solution for Be 15: $(V-M_V)_o = 12.4$ mag and $\log(\text{age}) = 8.5$, since they fit Be 15 to the B-type main-sequence stars of Schmidt-Kaler (1982) in the CC diagram. To discern between our solution for Be 15 and that of Lata et al. (2004) will require spectral types for the brighter stars, to determine whether they are G- or B-types. The methodology of Sujatha et al. (2004) employs the more independent $(B-I)$ vs $(B-V)$ technique given by Natali et al. (1994) for determining the interstellar

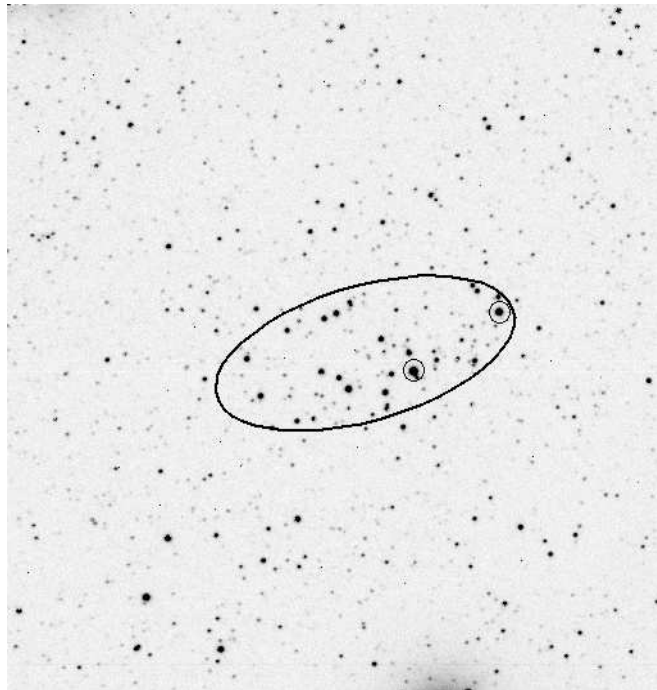


Figure 5. Visual image of the open cluster Be 80 from the DPSS. The ellipse encloses the region studied in this publication, and the two small circles mark the brightest two stars in this elliptical region. The second brightest is most surely a foreground star as seen in Figs 6, 8, and 9, while the brightest is that unusual star far to the right in Fig. 6. North is up, and east to the left in this presentation

reddening, and so provides confidence in our results for a small-reddening/small-distance/large-age solution for Be 15.

On the other hand, most recently Maciejewski & Niedzielski (2007) have also studied this cluster, but using only two-filter (BV) , wide-field CCD photometry with only a single CM diagram used to derive all the cluster parameters (distance modulus, reddening, and age) by means of χ^2 fitting to the solar-metallicity isochrones of Bertelli et al. (1994). It is obvious in the Be 15 panel of their Fig. 2 that their decontamination of the field of Be 15 has been only partially successful, due to the remaining presence of field red-giant stars and also anomalous stars which extend beyond the main sequence of this cluster. Maciejewski & Niedzielski obtain a large-reddening/large-distance/small-age solution for Be 15, similar to that of Lata et al. (2004): $E(B-V) = 1.01 \pm 0.15$ mag, $(V-M_V)_o = 12.15 \pm 0.4$ mag, and $\log(\text{age}) = 8.7 \pm 0.1$.

5 BERKELEY 80

This open cluster is located in the constellation Aquila, in the Galactic central region ($\ell, b = 32.18^\circ, -01.21^\circ$), has an apparent diameter of 3–4 arcmin (Dias et al. 2002; Lyngå 1987), was classified as II-2-p by Trumpler (1930) and reclassified as II-1-p by Lyngå (1987), indicating a poor cluster ($\lesssim 50$ stars) with a little central condensation, and a narrow to medium luminosity contrast with respect to the surrounding fields. Lyngå (1987) gives ≈ 15.0 mag as the visual magnitude of the brightest star. This cluster has also been

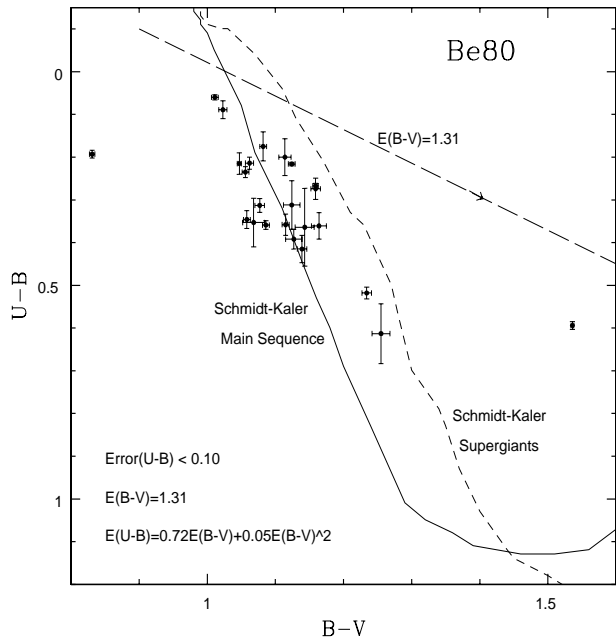


Figure 6. The CC, $(U-B)$ vs $(B-V)$, figure for the open cluster Be 80. This cluster has been fit to the main-sequence colours of Schmidt-Kaler (1982), the solid line from upper left to lower right; the mostly parallel short-dash line represents the supergiant colours of Schmidt-Kaler. Only stars with photometric errors less than 0.10 mag for the colour $(U-B)$ and within the ellipse defined in the text (Fig. 5) have been plotted. Photometric error bars, and the reddening vector corresponding to $E(B-V) = +1.31$ mag are also plotted (long-dashes). Due to the large interstellar reddening of Be 80, the second order term of $0.05E(B-V)^2$ has been included here in the reddening equation

designated as C 1851-013 in Simbad. Be 80 is about 2.5° from the Serpens Cauda dark band of the Milky Way, and contains the infrared source *IRAS*18518-0117 at the very southern edge of our elliptical study area (cf. Fig. 5); this IR source is the brightest object of our I images of Be 80, fourth brightest in the *R* images of the study area, quite faint in the visual ($V \approx 17.45$ mag), and essentially undetected in *B* and *U*. To improve the contrast and visibility of this cluster in the various CC and CM diagrams an elongated ellipse containing the central region of Be 80 has been defined with the macro ‘ellipse’ (see Fig. 5); this cluster appears very prolonged in all of its images: centre at (520,460) pixels, north-south axis 110 pixels (0.72 arcmin), east-west axis 240 pixels (1.58 arcmin), and a rotation of 105° , from north toward east.

5.1 Colour-colour diagram, $(U-B)$ versus $(B-V)$

The $(U-B)$ versus $(B-V)$ diagram of this open cluster is presented in Fig. 6 together with the Schmidt-Kaler (1982) main-sequence colours, which has been fit to the B-type stars providing an interstellar reddening of $E(B-V) = 1.31 \pm 0.05$ mag for Be 80. Only stars with photometric errors less than 0.10 mag for the colour $(U-B)$ have been plotted to compensate for the low sensitivity of this CCD in the ultraviolet, and only stars within the ellipse of Fig. 5 have been

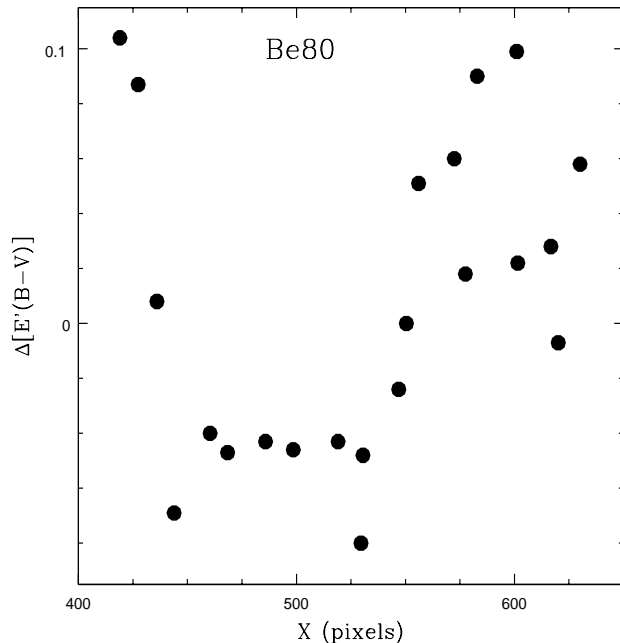


Figure 7. A measure of the scatter in Fig. 6 is plotted as a function of the star’s north-south position in pixels. The ordinate of this figure, $\Delta[E'(B-V)]$, is measured along a reddening vector from the Schmidt-Kaler main-sequence relation for B-type stars to each star’s position in the $(U-B)$ vs $(B-V)$ diagram of Fig. 6. Structure indicating variable interstellar extinction for Be 80 is clearly seen with an obvious minimum for the extinction over pixels 440-550

included. Photometric error bars, and the reddening vector corresponding to $E(B-V) = +1.31$ mag are also shown in Fig. 6. Due to the large interstellar reddening of this cluster, the reddening fit of Fig. 6 has been done with the equation $E(U-B) = 0.72E(B-V) + 0.05E(B-V)^2$, including the second-order term, which increases the final reddening value by about 0.03 mag. The points of Fig. 6 show considerable scatter about the Schmidt-Kaler main-sequence line suggesting variable interstellar extinction at this region of the sky as discussed in the next section.

Carraro et al. (2005) have also studied Be 80 using CCD *BVI* photometry and have estimated a reddening of $E(B-V) = 1.10 \pm 0.05$ mag by matching several CM diagrams with the same isochrones of Girardi et al. (2000). They apparently adjusted simultaneously for the reddening, distance modulus, and age in these CM diagrams, assuming also a solar metallicity. Since they did not observe Be 80 in the ultraviolet, they could not make use of the $(U-B, B-V)$ diagram as we have done here. Using Figs 5a and 6l from Neckel & Klare (1980) and a distance of 1.3–1.4 kpc (from Section 5.3 below, $V-M_V \cong 10.75$ mag), $A_V(r) \cong 4.0$ mag is estimated from their reddening maps, which agrees satisfactorily with our value of $A_V = 3.1E(B-V) = 4.06$ mag.

In Fig. 5 the two brightest stars of the ellipse are indicated with small circles. Star No. 1 is the brightest, falls at the lower centre of the ellipse, and far to the right in Fig. 6. Star No. 2 is the second brightest, is located at the right edge of the ellipse, and far to the left in Fig. 6. Star 2 is a foreground star with a smaller distance and less inter-

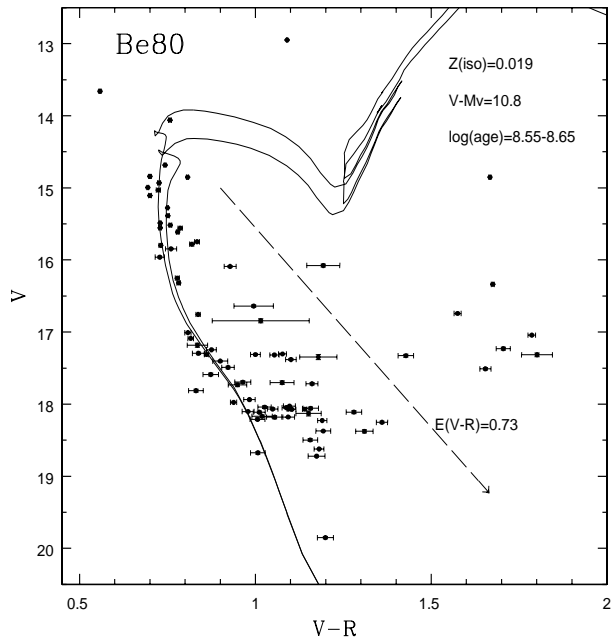


Figure 8. The CM figure, $(V, V-R)$, for the open cluster Be 80, which has been fit to the isochrones of Girardi et al. (2000) according to the interstellar reddening $E(B-V) = +1.31$ mag and a solar metallicity. The distance modulus has been determined by fitting vertically to the isochrones at the intermediate magnitudes of the main sequence, $16.5 \lesssim V \lesssim 18.0$ mag, and the age by fitting the turn-off at the brighter magnitudes, $14.0 \lesssim V \lesssim 16.0$. Photometric error bars, and the reddening vector corresponding to $E(B-V) = +1.31$ mag are also shown

stellar reddening than the cluster. The brightest, Star 1, is more difficult to explain; its position to the right in this CC diagram would suggest more interstellar reddening, but its brightness would suggest a foreground star.

5.2 Probable variable interstellar extinction

The reddening solution for Be 80 has been obtained by fitting the Schmidt-Kaler (1982) main-sequence colours to those 22 stars falling within the ellipse of this cluster's approximate shape (Fig. 5) and having the smaller photometric observing errors in the colour $(U-B)$ ($\sigma_{(U-B)} < 0.10$ mag), by assuming that these stars are B-type stars, and by excluding the two extreme stars mentioned above. This fit has given a large value for the interstellar reddening ($E(B-V) = 1.31$ mag), but the stars show a rather large scatter, ≈ 0.20 mag, about the Schmidt-Kaler line in this CC diagram (Fig. 6), suggesting variable interstellar, or intracluster, extinction across this object.

In Fig. 7 the scatter of this CC diagram, measured along a reddening vector, is plotted as a function of the north-south (or X-axis) position of a star in pixels. Structure is clearly seen with a minimum in the reddening for a band of pixels from about 440 to 550; this 0.72 arcmin band runs approximately east-west. To the north-west three stars have larger reddenings, and to the south-east 10 stars show increasing reddening with increasing pixel value. A plot of this scatter against Y, the east-west position in pixels, shows no

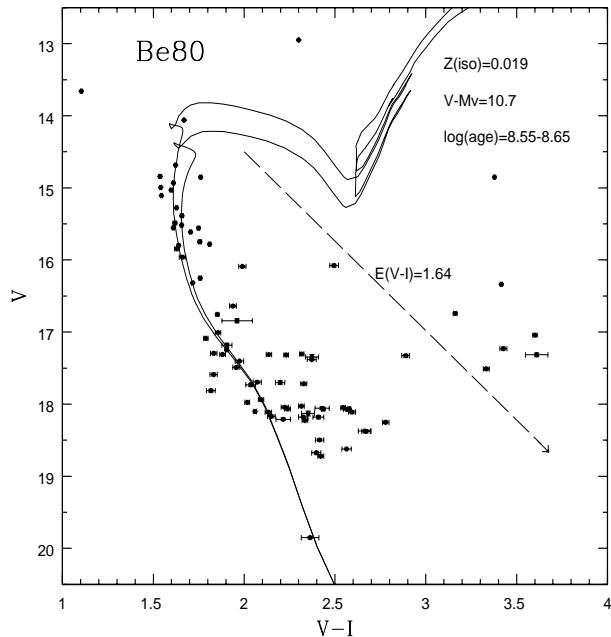


Figure 9. The CM figure, $(V, V-I)$, for the open cluster Be 80. This cluster has been fit to the isochrones of Girardi et al. (2000) using $E(B-V) = 1.31$ mag and a metallicity of $[Fe/H] = 0.00$ dex. Other details as in Fig. 8

clear structure. A colour plot against (X, Y) shows that this minimum in reddening runs approximately east-north-east to west-south-west, slightly skewed, $\approx 30^\circ$, with respect to the major axis of the elliptical study area, but many more stars with precise values of $E(B-V)$ are needed for any firm conclusions. The amplitude of this scatter in Fig. 7 is 0.184 mag, corresponding to $\Delta E(B-V) \cong 0.15$ mag, and $\Delta A_v \cong 0.46$ mag. This structure suggests the possibility that this cluster is a phantom cluster caused by an extinction minimum in the interstellar medium allowing us to see more background stars. However, the appearance of our CM diagrams for this region (in the next section) does indicate that there is an open cluster here, and CM diagrams from 2MASS (Skrutskie et al. 2006), such as $(K, K-J)$, also suggest the presence of a cluster. Only much deeper UBV CCD data for this region, providing many more stars with good errors in $(U-B)$ for mapping the interstellar extinction with better extent and spatial resolution, could help us to understand the variable interstellar absorption of this interesting region.

5.3 Colour-magnitude diagrams

In Figs 8 and 9 are shown two of the CM diagrams examined for Be 80 to determine its distance and age, the $(V, V-R)$ and the $(V, V-I)$, respectively. These redder CM diagrams have been preferred in order to mitigate the effects of the large and variable interstellar reddening of this cluster. In these diagrams the CCD observations of this cluster have been fit to the isochrones of Girardi et al. (2000) according to the interstellar reddening determined above $E(B-V) = 1.31$ mag, which converts to $A_v = 4.06$, $E(V-R) = 0.73$, and $E(V-I)$

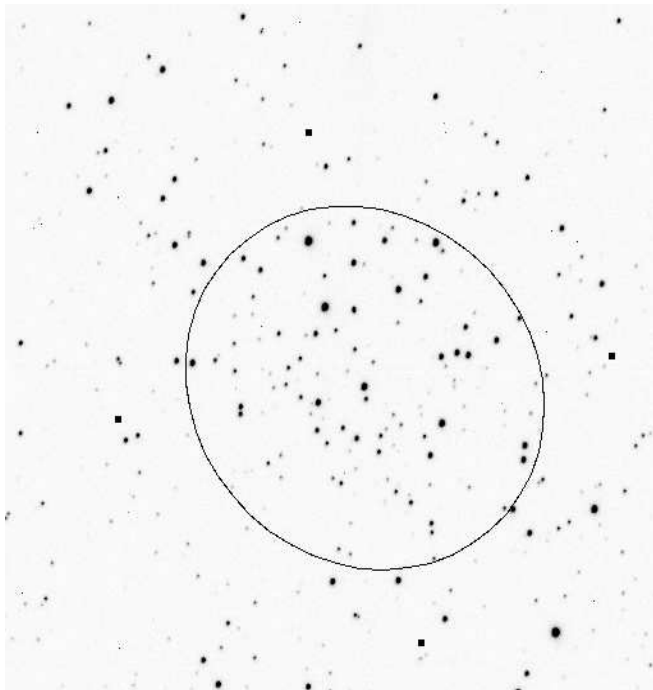


Figure 10. Visual image of the open cluster NGC 2192, as seen on the DPSS. The ellipse encloses the region studied in this publication. North is up and east to the left

I) = 1.64 mag, according to the reddening ratios of Straizys (1995), $E(V-R) = 0.56E(B-V)$ and $E(V-I) = 1.25E(B-V)$. Solar metallicity has been assumed, since F-type stars are not available for measuring an ultraviolet excess.

The distance moduli have been determined by shifting the reddening-corrected isochrones vertically to fit the observed V magnitudes at intermediate values, $16.5 \lesssim V \lesssim 18.0$ mag. The $(V, V-R)$ diagram provides a distance modulus of $(V-M_V)_o = 10.8$ mag, while the $(V, V-I)$ gives $(V-M_V)_o = 10.7$, both with uncertainties of ± 0.1 mag. Likewise, both diagrams have been used to estimate the cluster age by fitting the cluster turn-offs to the isochrones at the brighter magnitudes, $14.0 \lesssim V \lesssim 16.0$. Both the $(V, V-R)$ and $(V, V-I)$ diagrams give age estimates of $8.55 \lesssim \log(\text{age}) \lesssim 8.65$. Again two isochrones are plotted in each of the diagrams to give a feeling for the uncertainties involved here, and again the results from these two CM diagrams concerning the distance modulus and age are very consistent.

When comparing our results to those of Carraro et al. (2005), if we compare our **apparent** distance modulus of $V-M_V = 10.75 + A_V = 14.81 \pm 0.1$ mag to their apparent value of 14.8 ± 0.2 , an almost perfect agreement is found. So, the only difference is that between the two values for the interstellar reddening, $E(B-V) = +1.31$ mag (ours) and $+1.10$ (theirs).

6 NGC 2192

This open cluster is located in the constellation Auriga, in the Galactic anti-centre direction ($\ell, b = 173.42^\circ, +10.65^\circ$), has an apparent diameter of about 5.0 arcmin (Dias et al. 2002) and was classified as III-1-p by Trumpler (1930)

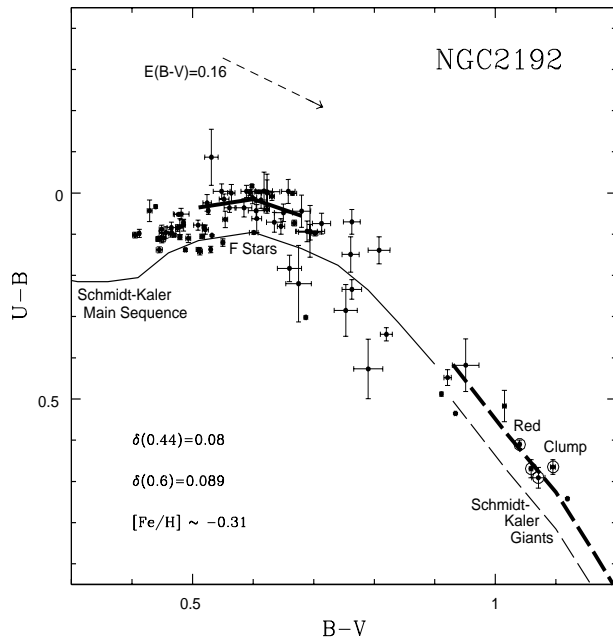


Figure 11. The CC, $(U-B)$ vs $(B-V)$, figure for the open cluster NGC 2192. This cluster has been fit to the main-sequence colours of Schmidt-Kaler (1982), the solid line from $(B-V) = +0.30$ to $+0.90$ mag, assuming an ultraviolet excess, $\delta(0.44) = 0.08$ mag, for the F-type cluster stars, represented by the thick solid line over $0.51 \leq (B-V) \leq 0.68$ mag; this fit gives $E(B-V) = +0.16 \pm 0.03$ for the interstellar reddening. At this same reddening the red-clump stars fit very well the red-giant (III) colours of Schmidt-Kaler, the dashed line over $(B-V) \geq 0.93$ mag, with a corresponding ultraviolet excess given by the thick dashed line. The reddening vector corresponding to $E(B-V) = +0.16$ mag is also shown

and reclassified as II-2-m by Lyngå (1987), indicating a medium to poor cluster ($\lesssim 50$ – 100 stars) with a little or no central condensation, and a narrow to medium luminosity contrast with respect to the surrounding fields. Lyngå (1987) gives 45 as the number of member stars, ≈ 14.0 mag as the visual magnitude of the brightest star, and 10.7 mag as the total visual magnitude of this cluster. This cluster has also been designated C 0611+398 and Cl Melotte 42 in Simbad. To concentrate on the central region in order to increase contrast with respect to the surrounding field, the awk macro ‘elipse’ has been applied to extract those stars centred at (570,460) pixels with an elliptical form of 260 pixels north-south (1.71 arcmin), 290 pixels east-west (1.90 arcmin), and a rotation of $+55^\circ$, from north toward east (see Fig. 10).

NGC 2192 is one of 72 open clusters having the most accurately determined parameters, selected by Paunzen & Netopil (2006) from a statistical analysis of 395 open clusters found in the literature with a total of 6437 estimates for their parameters. These 72 clusters serve as a standard list for future comparisons and tests between different isochrones and stellar models. The interstellar reddening, distance, and age derived for NGC 2192 by Paunzen & Netopil agree excellently with those of Park & Lee (1999), well within observational errors.

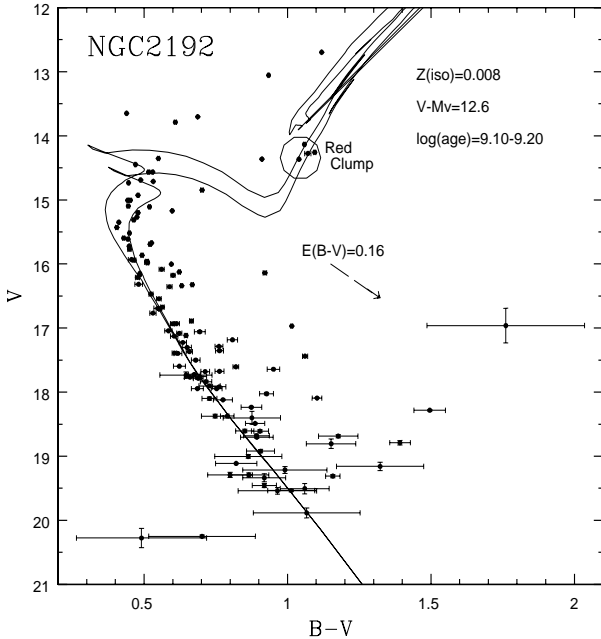


Figure 12. The CM figure, $(V, B-V)$, for the open cluster NGC 2192. This cluster has been fit to the isochrones of Girardi et al. (2000) according to $E(B-V) = +0.16$ mag and $[Fe/H] = -0.31$ dex. The distance modulus has been determined by shifting vertically the cluster to the isochrones at the intermediate magnitudes of the main sequence, $17.0 \lesssim V \lesssim 18.5$ mag, and the age by fitting the turn-off of the cluster at the brighter magnitudes, $14.5 \lesssim V \lesssim 16.5$. Photometric error bars, the position of the red-clump stars, and the reddening vector corresponding to $E(B-V) = 0.16$ mag are also shown

6.1 Colour-colour diagram, $(U-B)$ versus $(B-V)$

The $(U-B)$ versus $(B-V)$ diagram of this open cluster allows a nicely consistent fit for both the interstellar reddening and the metallicity using simultaneously the F-type stars and the red-clump stars (cf. Fig. 11). The Schmidt-Kaler (1982) main-sequence colours are fit to the F-type stars with the same interstellar reddening, $E(B-V) = 0.16 \pm 0.03$ mag, as used to fit the red-clump stars to the Schmidt-Kaler giant colours. However, there is one complication in that the best fit between the F-type stars and the Schmidt-Kaler main sequence occurs for a slight ultraviolet excess of $\delta(0.44) = +0.08$ mag, but this value agrees very well with the resulting ultraviolet excess at the red-clump stars when compared to the Schmidt-Kaler giant colours for this same interstellar reddening. The resulting red-clump ultraviolet excess of $\delta(B-V) \approx +0.09$ mag agrees very well with that seen at the F-type stars according to the normalization of these excesses as a function of $B-V$, given in Table 1A of Sandage (1969). The top of the F-star hump for the Schmidt-Kaler $(U-B)$ vs $(B-V)$ relation corresponds to $(B-V) = +0.44$ mag (unreddened), while the red-clump stars to $(B-V) \approx +0.90$ mag (unreddened). According to Table 1A of Sandage both excesses correct to $\delta(0.6) \approx +0.089$ mag at $(B-V) = +0.60$ mag, which is that $(B-V)$ value at which most $[Fe/H]$ calibrations of the $UBV(RI)_C$ photometric system have been made. From equation (8) of Karataş & Schus-

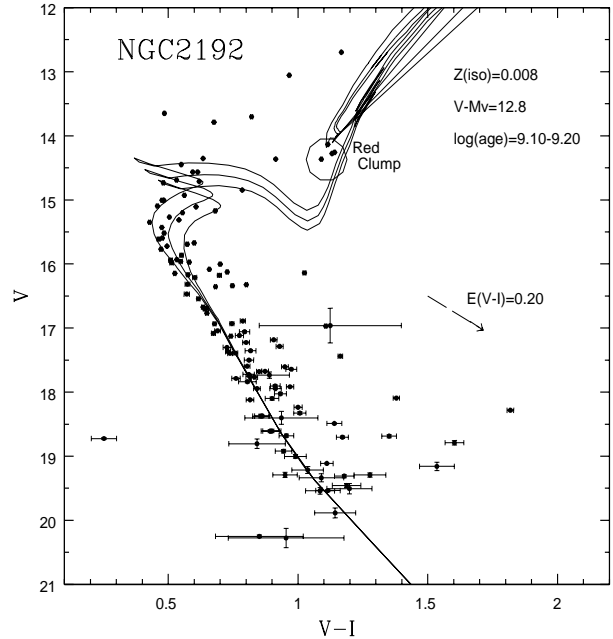


Figure 13. The CM figure, $(V, V-I)$, for the open cluster NGC 2192. This cluster has been fit to the isochrones of Girardi et al. (2000) according to $E(B-V) = +0.16$ mag and $[Fe/H] = -0.31$ dex, derived above. Other details as in Fig. 12

ter (2006), $\delta(0.6) = +0.089$ mag gives $[Fe/H] = -0.31 \pm 0.05$ dex for NGC 2192, which agrees excellently with the $[Fe/H]$ derived from the $\delta(0.6)$, $[Fe/H]$ calibration of Sandage & Fouts (1987), also $[Fe/H] = -0.31$. Park & Lee (1999) in their CCD $UBVI$ study of NGC 2192 have also obtained $[Fe/H] = -0.31 \pm 0.15$ dex, making use of this same $(U-B)$ vs $(B-V)$ diagram.

6.2 Colour-magnitude diagrams

Figs 12 and 13 show two of the CM diagrams examined to determine the distance and age for NGC 2192, the $(V, B-V)$ and the $(V, V-I)$, respectively. In these diagrams the observations have been fit to the isochrones of Girardi et al. (2000) according to the $E(B-V) = +0.16$ mag and $[Fe/H] = -0.31$ dex ($Z = 0.008$) obtained in Section 6.1. $E(B-V) = +0.16$ mag converts to $A_v = 0.496$ mag and $E(V-I) = +0.20$ mag, according to the reddening ratios found in Straizys (1995).

For both CM diagrams of Figs. 12 and 13, the distance moduli have been determined by shifting the reddening-corrected isochrones vertically until they fit the observed V magnitudes at intermediate values, $17.0 \lesssim V \lesssim 18.5$ mag. The $(V, B-V)$ and $(V, V-I)$ diagrams give distance moduli of $(V-M_V)_o = 12.6$ mag and 12.8, respectively. Likewise, both CM diagrams have been used to estimate the cluster ages by fitting the cluster turn-offs to the isochrones at the brighter magnitudes, $14.5 \lesssim V \lesssim 16.5$. Both diagrams indicate a cluster age in the range, $9.10 \lesssim \log(\text{age}) \lesssim 9.20$ as shown by the multiple isochrones plotted: $\log(\text{age}) = 9.10, 9.15$, and 9.20; these multiple isochrones also help to estimate the uncertainties in these (logarithmic) age estimates, $\approx \pm 0.05$ dex. These ages of $\log(\text{age}) \approx 9.10-9.20$ also provide a fairly

good fit to the red-clump stars, as seen in both figures. Also, our values for the distance modulus and age of NGC 2192 agree very well, within the estimated observational errors, with those derived by Park & Lee (1999): 12.7 ± 0.2 mag and 9.04 ± 0.06 , respectively.

Maciejewski & Niedzielski (2007) have also studied NGC 2192 using wide-field BV CCD photometry and only a single CM diagram ($V, B-V$) to obtain the interstellar reddening, distance modulus, and age using a χ^2 fitting to the solar metallicity isochrones of Bertelli et al. (1994). In the NGC 2192 panel of their Fig. 2, it is clear that their decontamination procedure has worked much better for this cluster. Due to the differences in metallicity and procedure, they have obtained cluster parameters different from those of this paper and of Park & Lee (1999): $E(B-V) = 0.04 \pm 0.13$ mag, $(V-M_V)_o = 12.0 \pm 0.5$ mag, and $\log(\text{age}) = 9.3 \pm 0.1$.

7 DISCUSSION AND CONCLUSIONS

In Table 4 are summarized the results from this study. When the San Pedro Mártir open cluster survey began, only the cluster NGC 2192 had previous studies (Park & Lee 1999), but in the meantime three studies for Be 15 (Sujatha et al. 2004; Lata et al. 2004; Maciejewski & Niedzielski 2007) have appeared as well as one for Be 80 (Carraro et al. 2005), and another for NGC 2192 (Maciejewski & Niedzielski 2007). Our results for NGC 2192 agree well with those from Park & Lee for all parameters: reddening, metallicity, distance, and age, as can be seen in Table 4; but we disagree somewhat with Maciejewski & Niedzielski (2007) due to a difference in the assumed metallicity (they assume $Z = 0.019$) and due to their use of only a single CM diagram to derive all parameters, i.e. no CC diagram to estimate the interstellar reddening. For Be 15 our results agree fairly well with those of Sujatha et al. (2004) despite a difference in our derived reddening. Our results do not agree with those from Lata et al. (2004) and Maciejewski & Niedzielski (2007) due mainly to the fact that they fit the main sequence to early-type, main-sequence colours, while we have fit to the G-type, main-sequence colours of Schmidt-Kaler (1982). For Be 80 our **apparent** distance modulus and age agree very well with those from Carraro et al. (2005), but our distances do not agree, mainly due to differing values for the interstellar reddening. They have fit isochrones of Girardi et al. (2000) to several CM diagrams from BVI photometry to estimate simultaneously the distance modulus, reddening, and age, while we have used the $(U-B, B-V)$ diagram to separate the reddening solution from that for the distance modulus and age, providing a more independent and reliable result.

7.1 Conclusions

(i) Our best values for the interstellar reddening, distance modulus, and $\log(\text{age})$ for Be 15 are $E(B-V) = 0.23 \pm 0.03$ mag, $(V-M_V)_o = 10.4 \pm 0.1$ mag, and $\log(\text{age}) \cong 9.35 \pm 0.05$ mag or 9.95 ± 0.05 , respectively. The two possible solutions for the cluster age of Be 15 depend upon the membership, or no, of the three brightest stars, as seen in Figs 3 and 4.

(ii) Our results for Be 15 agree well with those of Sujatha et al. (2004), who employ the more independent $(B-I)$ vs $(B-V)$ technique given by Natali et al. (1994) for de-

termining the interstellar reddening, but do not agree well with the results of Lata et al. (2004) nor with those of Maciejewski & Niedzielski (2007); the former have fit the main-sequence stars of Be 15 to the B-type, main-sequence colours of Schmidt-Kaler (1982), while the latter to the early-type isochrones of Bertelli et al. (1994); we have fit Be 15 to the G-type, main-sequence colours of Schmidt-Kaler. This suggests the need for spectroscopy for the brighter stars of Be 15 to determine the membership of the brightest stars using radial velocity measurements, and spectral-type classifications to know whether the brighter members are in fact G-types or B-types.

(iii) Our best values for the interstellar reddening, distance modulus, and $\log(\text{age})$ for Be 80 are $E(B-V) = 1.31 \pm 0.05$ mag, $(V-M_V)_o = 10.75 \pm 0.1$ mag, and $\log(\text{age}) \cong 8.60 \pm 0.05$, respectively. Our value for the reddening is in good agreement with that derived from the extinction maps of Neckel & Klare (1980). Our **apparent** distance modulus and age agree very well with the values of Carraro, the main difference between our solutions is the interstellar reddening; they obtain $E(B-V) = 1.10 \pm 0.05$ mag.

(iv) Clear evidence for variability of the interstellar extinction across the face of the open cluster Be 80 has been detected. The maximum of this change occurs approximately in the north-south direction, and the reddening has a minimum with a width of about 0.72 arcmin, running approximately east-north-east to west-south-west, slightly north of the cluster's centre, and slightly skewed, $\approx 30^\circ$, with respect to the major axis of our elliptical study area. Much deeper CCD $UBV(RI)_C$ photometry is recommended to map more thoroughly the interstellar extinction in the vicinity of Be 80 and to study the structure of the interstellar, or intracluster, reddening of this interesting region.

(v) A very consistent and simultaneous solution for the interstellar reddening and metallicity of NGC 2192, $E(B-V) = +0.16 \pm 0.03$ mag and $[Fe/H] = -0.31 \pm 0.05$, is obtained from the CC $(U-B, B-V)$ diagram using both the F-type and the red-clump stars. Park & Lee (1999) obtained this identical metallicity by means of a similar study using CCD $UBVI$ photometry; they obtained a slightly larger reddening of $E(B-V) = +0.20 \pm 0.03$ mag. Our distance modulus for NGC 2192, $(V-M_V)_o = 12.7 \pm 0.1$ mag, from Figs 12 and 13, agrees very well with that from Park & Lee (1999), $(V-M_V)_o = 12.7 \pm 0.2$ mag. The ages also agree within the quoted errors, $\log(\text{age}) = 9.15 \pm 0.05$ from this paper, and $\log(\text{age}) = 9.04 \pm 0.06$ from Park & Lee.

(vi) Our results for NGC 2192 do not agree as well with those from Maciejewski & Niedzielski (2007), but they use only a single CM diagram ($V, B-V$) to estimate all cluster parameters, i.e. no CC diagram for the interstellar reddening, and assume a solar metallicity for the isochrones.

ACKNOWLEDGMENTS

We wish to thank the staff of the San Pedro Mártir Observatory for their help with the CCD observations, and also we greatly appreciated the participation of C.A. Santos, and J. McFarland, who assisted with the data reductions and programming. This research made use of the WEBDA open cluster database of J.-C. Mermilliod. This work was sup-

Table 4. The inferred fundamental parameters of the three open clusters. The cluster name and Galactic coordinates are presented in Columns 1 and 2, respectively. The derived reddening $E(B-V)$ together with its uncertainty is given in Column 3, and the metallicity and heavy-element abundances, $[Fe/H]$ and Z , in Columns 4 and 5, respectively. The average values of the distance modulus, $(V-M_V)_o$, heliocentric distance (pc), and $\log(\text{age})$ (age in yrs), together with their uncertainties, are listed in Columns 6, 7, and 8, respectively. The corresponding references from the literature are shown in Column 9.

Cluster	(ℓ°, b°)	$E(B-V)$ (mag)	$[Fe/H]$ (dex)	Z	$(V-M_V)_o$ (mag)	$d(\text{pc})$	$\log(\text{age})(\text{age in yrs})$	Reference
Be 15	162.33, +1.61	0.23 ± 0.03	0.00	+0.019	10.4 ± 0.1	1202	9.35, or 9.95 ± 0.05	This paper
		0.462	–	solar	10.5	1259	9.7	Sujatha et al. (2004)
		0.88 ± 0.05	–	solar	12.4 ± 0.2	3051	8.5 ± 0.1	Lata et al. (2004)
		1.01 ± 0.15	–	solar	12.15 ± 0.4	2690	8.7 ± 0.1	Maciejewski &... (2007)
Be 80	32.17, +1.25	1.31 ± 0.05	0.00	+0.019	10.75 ± 0.1	1413	8.6 ± 0.05	This paper
		1.10 ± 0.05	–	solar	11.39 ± 0.2	1897	8.5 ± 0.15	Carraro et al. (2005)
NGC 2192	173.41, +10.64	0.16 ± 0.03	-0.31	+0.008	12.7 ± 0.1	3467	9.15 ± 0.05	This paper
		0.20 ± 0.03	-0.31	+0.009	12.7 ± 0.2	3467	9.04 ± 0.06	Park & Lee (1999)
		0.04 ± 0.13	–	solar	12.0 ± 0.5	2500	9.3 ± 0.1	Maciejewski &... (2007)

ported by the CONACyT projects 33940, 45014, 49434 and PAPIIT-UNAM IN111500 (México).

REFERENCES

- Arce H.G., Goodman A.A., 1999, *ApJ*, 512, L135
 Becker W., Fenkart R.B., 1970, in Becker W., Contopoulos, G.I., eds, *The Spiral Structure of Our Galaxy*, IAU Symposium 38, Reidel, Dordrecht, p. 205
 Bertelli G., Bressan A., Chiosi C., Fagotto F., Nasi E., 1994, *A&A*, 106, 275
 Bonifacio P., Monai S., Beers T.C., 2000, *AJ*, 120, 2065
 Cabrera-Canño J., Polvorinos E.J., Alfaro A., 1990, in Jaschek C., Murtagh F., eds, *Errors, Bias, and Uncertainties in Astronomy*, Cambridge Univ. Press, Cambridge
 Carraro G., Ng Y.K., Portinari L., 1998, *MNRAS*, 296, 1045
 Carraro G., Janes K.A., Eastman J.D., 2005, *MNRAS*, 364, 179
 Chavarría-K C., 1994, *RevMexA&A*, 29, 137
 Dias W.S., Alessi B.S., Moitinho A., Lépine J.R.D., 2002, *A&A*, 389, 871
 Feinstein A., 1994, *RevMexA&A*, 29, 141
 Friel E.D., 1995, *ARA&A*, 33, 381
 Girardi L., Bressan A., Bertelli G., Chiosi C., 2000, *A&AS*, 141, 371
 Howell S.B., 1989, *PASP*, 101, 616
 Howell S.B., 1990, in *ASP Conf. Ser. 8, CCDs in Astronomy*, ed. G.H. Jacoby (San Francisco: ASP), 312
 Janes K.A., 1979, *ApJS*, 39, 135
 Janes K.A., Adler D., 1982, *ApJS*, 49, 425
 Karataş Y., Schuster W.J. 2006, *MNRAS*, 371, 1793
 Kassis M., Janes K.A., Friel E.D., Phelps R.L., 1997, *AJ*, 113, 1723
 Landolt A.U., 1983, *AJ*, 88, 439
 Landolt A.U., 1992, *AJ*, 104, 340
 Lata S., Mohan V., Sagar R., 2004, *Bull. Astr. Soc. India*, 32, 371
 Lyngå G., 1987, *Computer Based Catalogue of Open Cluster Data*, Observatoire de Strasbourg, Centre de Données Stellaires, Strasbourg
 Maciejewski G., Niedzielski A., 2007, *A&A*, 467, 1065
 McFarland J., 2009, BSc Thesis, Universidad Autónoma de Baja California, México
 Mermilliod J.-C., 1982a, *A&A*, 109, 37
 Mermilliod J.-C., 1982b, *A&A*, 109, 48
 Mermilliod J.-C., Mayor M., 1989, *A&A*, 219, 125
 Meynet G., Mermilliod J.-C., Maeder A., 1993, *A&AS*, 98, 477
 Michaud G., Richard O., Richer J., Vandenberg D.A., 2004, *ApJ*, 606, 452
 Moffat A.F.J., Vogt N., 1973, *A&A*, 23, 317
 Moitinho A., 2001, *A&A*, 370, 436
 Moitinho A., 2002, in Grebel E.K., Brandner W., eds, *Modes of Star Formation and the Origin of Field Populations*, ASP Conference Proceedings, Vol. 285, Astronomical Society of the Pacific, San Francisco
 Moitinho A., Alves J., Huéramo N., Lada C.J., 2001, *ApJL*, 563, L93
 Natali F., Natali G., Pompei E., Pedichini F., 1994, *A&A*, 289, 756
 Neckel Th., Klare G., 1980, *A&AS*, 42, 251
 Park H.S., Lee M.G., 1999, *MNRAS*, 304, 883
 Paunzen E., Netopil M., 2006, *MNRAS*, 371, 1641
 Phelps R.J., Janes K.A., 1994, *ApJS*, 90, 31
 Piatti A.E., Claria J.J., Abadi M.G., 1995, *AJ*, 110, 2813
 Sandage A., 1969, *ApJ*, 158, 1115
 Sandage A., Fouts G., 1987, *AJ*, 93, 74
 Schlegel D.J., Finkbeiner D.P., Davis M., 1998, *ApJ*, 500, 525 (SFD)
 Schmidt-Kaler Th., 1982, in Schaifers K., Voigt H.H., eds., *Landolt-Börnstein: Numerical Data and Functional Relationships in Science and Technology - New Series, Group VI, Vol. 2(b)*, Springer-Verlag, Berlin
 Schuster W.J., Beers T.C., Michel R., Nissen P.E., García G., 2004, *A&A*, 422, 527
 Schuster W., Michel R., Dias W., Tapia-Peralta T., Vázquez R., Macfarland J., Chavarría C., Santos C., & Moitinho, A., 2007, *Galaxy Evolution Across the Hubble Time*, eds. F. Combes and J. Palouš, *Proceedings of the International Astronomical Union, IAU Symposium No. 235*, (Cambridge, United Kingdom: Cambridge University Press), p. 331
 Skrutskie M.F., Cutri R.M., Stiening R., Weinberg M.D., Schneider S., et al., 2006, *AJ*, 131, 1163
 Stetson, P.B., 1987, *PASP*, 99, 191
 Stetson, P.B., 1990, *PASP*, 102, 932
 Straizys, V., 1995, *Multicolor Stellar Photometry, Astronomy and Astrophysics Series, Vol. 15*, ed. A.G. Pacholczyk

(Tucson, Arizona: Pachart Pub. House)

Sujatha S., Babu G.S.D., Ananthamurthy S., 2004, Bull. Astr. Soc. India, 32, 295

Tapia-Peralta M.T., 2007, BSc Thesis, Universidad Autónoma de Baja California, México

Trumpler, R.J., 1930, Lick Obs. Bull., XIX (14), 154

Twarog B.A., Ashman K.M., Anthony-Twarog B.J., 1997, AJ, 114, 2556

SUPPORTING INFORMATION

Additional Supporting Information may be found in the online version of this article:

Table 1. Standard *UBVRI* CCD photometry and observing errors for the open cluster Be 15.

Table 2. The same as Table 1 but for Be 80.

Table 3. The same as Table 1 but for NGC 2192.